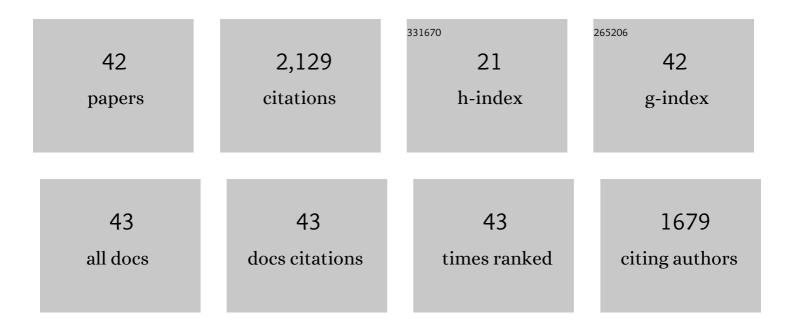
## Jun-Xi Zhang

List of Publications by Year in descending order

Source: https://exaly.com/author-pdf/983883/publications.pdf Version: 2024-02-01



#	Article	IF	CITATIONS
1	An air-stable iron/manganese-based phosphate cathode for high performance sodium-ion batteries. Chemical Engineering Journal, 2022, 433, 133798.	12.7	13
2	In situ micro-current collector of amorphous manganese dioxide as cathode material for sodium-ion batteries. Ionics, 2022, 28, 1211-1217.	2.4	2
3	Galvanic Effect and Alternating Current Corrosion of Steel in Acidic Red Soil. Metals, 2022, 12, 296.	2.3	2
4	The Study of Graphene Oxide on the Regulations and Controls of the Sol-Gel Film Structure and Its Performance. Metals, 2022, 12, 20.	2.3	5
5	K+-stabilized nanostructured amorphous manganese dioxide: excellent electrochemical properties as cathode material for sodium-ion batteries. Ionics, 2021, 27, 1559-1567.	2.4	7
6	Electrochemical properties of mixed-phosphates Nax+2Fex+1(PO4)x(P2O7) with different ratios of PO43-/P2O74 Journal of Alloys and Compounds, 2021, 870, 159382.	5.5	13
7	Facile Synthesis Strategy from Sludge-Derived Extracellular Polymeric Substances to Nitrogen-Doped Graphene Oxide-Like Material and Quantum Dots. ACS Omega, 2021, 6, 24940-24948.	3.5	4
8	Corrosion Behavior of Selective Laser Melted AlSi10Mg Alloy in NaCl Solution and Its Dependence on Heat Treatment. Acta Metallurgica Sinica (English Letters), 2020, 33, 327-337.	2.9	30
9	MCNT-Reinforced Na3Fe2(PO4)3 as Cathode Material for Sodium-Ion Batteries. Arabian Journal for Science and Engineering, 2020, 45, 143-151.	3.0	14
10	Highly Stable Na <sub>3</sub> Fe <sub>2</sub> (PO <sub>4</sub> ) <sub>3</sub> @Hard Carbon Sodium-Ion Full Cell for Low-Cost Energy Storage. ACS Sustainable Chemistry and Engineering, 2020, 8, 1380-1387.	6.7	44
11	A New Polyanion Na <sub>3</sub> Fe <sub>2</sub> (PO <sub>4</sub> )P <sub>2</sub> O <sub>7</sub> Cathode with High Electrochemical Performance for Sodium-Ion Batteries. ACS Energy Letters, 2020, 5, 3788-3796.	17.4	62
12	Galvanic Corrosion Behavior of Copper–Drawn Steel for Grounding Grids in the Acidic Red Soil Simulated Solution. Acta Metallurgica Sinica (English Letters), 2020, 33, 1571-1582.	2.9	8
13	Scalable synthesizing nanospherical Na4Fe3(PO4)2(P2O7) growing on MCNTs as a high-performance cathode material for sodium-ion batteries. Journal of Power Sources, 2020, 461, 228130.	7.8	55
14	The Suppression of transformation of γ-FeOOH to α-FeOOH accelerating the steel corrosion in simulated industrial atmospheric environment with a DC electric field interference. Corrosion Engineering Science and Technology, 2019, 54, 249-256.	1.4	12
15	Abnormal corrosion behavior of selective laser melted AlSi10Mg alloy induced by heat treatment at 300â∈ °C. Journal of Alloys and Compounds, 2019, 803, 314-324.	5.5	46
16	On the microstructure and corrosion behaviors of selective laser melted CP-Ti and Ti-6Al-4V alloy in Hank's artificial body fluid. Materials Research Express, 2019, 6, 126521.	1.6	18
17	Effect of direct current electric field intensity and electrolyte layer thickness on oxygen reduction in simulated atmospheric environment. Corrosion Science, 2019, 148, 206-212.	6.6	10
18	Resemblance in Corrosion Behavior of Selective Laser Melted and Traditional Monolithic β Ti-24Nb-4Zr-8Sn Alloy. ACS Biomaterials Science and Engineering, 2019, 5, 1141-1149.	5.2	75

Jun-Xi Zhang

#	Article	IF	CITATIONS
19	Sol-gel synthesis of porous Na3Fe2(PO4)3 with enhanced sodium-ion storage capability. Ionics, 2019, 25, 1083-1090.	2.4	24
20	K-doped Na3Fe2(PO4)3 cathode materials with high-stable structure for sodium-ion stored energy battery. Journal of Alloys and Compounds, 2019, 784, 939-946.	5.5	37
21	Distinction of corrosion resistance of selective laser melted Al-12Si alloy on different planes. Journal of Alloys and Compounds, 2018, 747, 648-658.	5.5	80
22	Improved corrosion behavior of ultrafine-grained eutectic Al-12Si alloy produced by selective laser melting. Materials and Design, 2018, 146, 239-248.	7.0	101
23	Probing the corrosion mechanism of zinc under direct current electric field. Materials Chemistry and Physics, 2018, 206, 232-242.	4.0	16
24	Influence of Direct Current Electric Field on Electrode Process of Carbon Steel under Thin Electrolyte Layers. Journal of the Electrochemical Society, 2018, 165, C385-C394.	2.9	3
25	The corrosion behavior of steel exposed to a DC electric field in the simulated wet-dry cyclic environment. Materials Chemistry and Physics, 2017, 192, 190-197.	4.0	18
26	Corrosion Behaviour of Selective Laser Melted Ti-TiB Biocomposite in Simulated Body Fluid. Electrochimica Acta, 2017, 232, 89-97.	5.2	166
27	Amorphous <scp>MnO<sub>2</sub></scp> as Cathode Material for Sodiumâ€ion Batteries. Chinese Journal of Chemistry, 2017, 35, 1294-1298.	4.9	29
28	Heat Treatment Degrading the Corrosion Resistance of Selective Laser Melted Ti-6Al-4V Alloy. Journal of the Electrochemical Society, 2017, 164, C428-C434.	2.9	112
29	Monoclinic Phase Na <sub>3</sub> Fe <sub>2</sub> (PO <sub>4</sub> ) <sub>3</sub> : Synthesis, Structure, and Electrochemical Performance as Cathode Material in Sodium-Ion Batteries. ACS Sustainable Chemistry and Engineering, 2017, 5, 1306-1314.	6.7	81
30	Electrochemical and SVET Studies on the Typical Polarity Reversal of Cu–304 Stainless Steel Galvanic Couple in Clâ^·Containing Solution with Different pH. Electrochimica Acta, 2017, 247, 207-215.	5.2	21
31	Fretting Wear Behaviors of Aluminum Cable Steel Reinforced (ACSR) Conductors in High-Voltage Transmission Line. Metals, 2017, 7, 373.	2.3	17
32	The relation between the structure and electrochemical performance of sodiated iron phosphate in sodium-ion batteries. Journal of Power Sources, 2016, 314, 1-9.	7.8	32
33	Influence of Direct Current Electric Field on the Formation, Composition and Microstructure of Corrosion Products Formed on the Steel in Simulated Marine Atmospheric Environment. Acta Metallurgica Sinica (English Letters), 2016, 29, 373-381.	2.9	14
34	Distinction in corrosion resistance of selective laser melted Ti-6Al-4V alloy on different planes. Corrosion Science, 2016, 111, 703-710.	6.6	325
35	Amorphous iron phosphate/carbonized polyaniline nanorods composite as cathode material in sodium-ion batteries. Journal of Solid State Electrochemistry, 2016, 20, 479-487.	2.5	15
36	Corrosion behavior of selective laser melted Ti-6Al-4 V alloy in NaCl solution. Corrosion Science, 2016, 102, 484-489.	6.6	401

Jun-Xi Zhang

#	Article	IF	CITATIONS
37	Direct growth of FePO <sub>4</sub> /reduced graphene oxide nanosheet composites for the sodium-ion battery. Journal of Materials Chemistry A, 2015, 3, 5501-5508.	10.3	47
38	The transformation from amorphous iron phosphate to sodium iron phosphate in sodium-ion batteries. Physical Chemistry Chemical Physics, 2015, 17, 22144-22151.	2.8	16
39	Effect of the direct current electric field on the initial corrosion of steel in simulated industrial atmospheric environment. Corrosion Science, 2015, 99, 295-303.	6.6	51
40	A maize-like FePO <sub>4</sub> @MCNT nanowire composite for sodium-ion batteries via a microemulsion technique. Journal of Materials Chemistry A, 2014, 2, 7221-7228.	10.3	58
41	Preparation and magnetic properties of Mn-Zn ferrites by the Co-precipitation method. Journal Wuhan University of Technology, Materials Science Edition, 2009, 24, 875-878.	1.0	7
42	The corrosion and passivation of SS304 stainless steel under square wave electric field. Materials Chemistry and Physics, 2003, 79, 43-48.	4.0	38